ADSORPTION OF SULFUR HEXAFLUORIDE ON 13X ZEOLITE MODIFIED BY METAL CATION EXCHANGE

Tran Hoai Lam[1*], Quach Nguyen Khanh Nguyen[2]
[1]*Ho Chi Minh City University of Food Industry*
[2]*Saigon University*
*Email: *thlam01@cntp.edu.vn*
Received: 19 December 2017; Accepted for publication: 5 June 2018

ABSTRACT

The sodium cations of 13X zeolite were replaced by Zn^{2+}, Co^{2+}, Ni^{2+} and Cu^{2+} cations contained in the various concentration of nitrate salts solutions. XRD and SEM analysis shows that the cationic exchange process is accompanied by a textural damage for the cation-exchanged 13X zeolites, especially, in the case of Ni^{2+} and Cu^{2+}-exchanged 13X zeolites. Investigation of SF_6 adsorption indicates that the SF_6 removal efficiency and quantity adsorbed depend on the metal cations, the concentration of nitrate salts solution, the SF_6 concentration as well as the rate of SF_6 flow. In which, the SF_6 removal efficiency is only obtained 99% for the Co^{2+}, Zn^{2+}-exchanged zeolites, and the highest SF_6 adsorbed quantity is 1.34 mg/g for 0.03CoX exchanged zeolite and 0.827 mg/g for 0.05ZnX exchanged zeolite, respectively.

Keywords: Sulfur hexafluoride, 13X zeolite, ion-exchange, adsorption, modified.

1. INTRODUCTION

Sulfur hexafluoride (SF_6) is an inorganic, colorless, odorless, non-flammable and heavy gas with characteristics such as relatively low toxicity, high thermal stability, extreme inertness and high dielectrics. Therefore, it is widely used in the electrical industry, semiconductor, aluminum smelting and magnesium industries, as well as medical applications such as the ultrasonography and in ophthalmologic surgeries [1–3]. However, the extremely stable natures of the SF_6 molecules with long lifetimes in the atmosphere of 3200 years and its high efficiency as infrared absorbers make it become to the very powerful greenhouse gas. The high global warming potential SF_6 is 22800 times more potent than CO_2 in terms of their capabilities to trap heat in the atmosphere over a hundred year period [4].

Hence, the efficient methods have been suggested as a necessary method for handling, recovering and storing the SF_6 gas, released from the industrial processes, such as the pressure swing adsorption, membrane separation, thermal swing adsorption etc. In which the selection of porous materials also affects significantly the efficiency of these adsorption-based processes. Up to now, some studies have reported about the adsorption and the separation of SF_6 with using carbon nanotube, graphene and titanium-graphene, metal-organic frameworks and zeolites [5–12]. That pore diameter of the porous material was also suggested approximately 11 Å is optimal for SF_6/N_2 selectivity [13].

D.V. Cao and S. Sircar pointed that the heat of SF_6 adsorption increases with increasing adsorbate loading on the NaX zeolites in the high coverage region, so the SF_6 adsorption efficiency on the NaX zeolites are decreased [12]. In order to overcome this problem, the

modification of zeolites was also proposed to improve adsorption capacity of zeolites due to the change of surface characteristic. It was known that the 13X zeolite is a high polar crystalline adsorbent. The 13X zeolite structure is a faujasite framework with a cage comprising SiO_4 and AlO_4 tetrahedra bound by bridged oxygen atoms to make a 12-ring pore openings, and 3-dimensional channel system and the diameter of the cavity in zeolite FAU is 13 Angstrom. The negative charges of the AlO_4 units are balanced by sodium cations that can be easily exchanged by other metal ions such as Ni^{2+}, Cr^{3+}, Zn^{2+}, Cu^{2+}, Co^{2+} [14–17]. Most of these reports indicated that the external surface area increase with increasing the amount of Na^+ ions, replaced by other metal ions. Besides, the pore diameter of exchanged 13X zeolite was also smaller than the raw 13X zeolite. Thus, SF_6 adsorption capacity and selectivity of the exchanged zeolites are better than the raw zeolites [13].

In this work, the sodium cations of 13X zeolite were replaced by Zn^{2+}, Co^{2+}, Ni^{2+} and Cu^{2+} ions in the various concentrations of nitrate salt solutions. The atomic components and characterization of the exchanged 13X zeolites were investigated by using XRD, SEM, EDS, BET and BJH methods. In addition, the effect of the metal ions, the initial solution concentration, the SF_6 concentration and rate of SF_6 flow on the SF_6 adsorption of exchanged 13X zeolites is also represented in this report.

2. MATERIALS AND EXPERIMENT

2.1. Materials

13X zeolites: is the spherical tablets with diameter, ~3.0 - 3.5 mm; 99% purity, Forever Applied Equipment Co., Ltd.; $Me(NO_3)_2$**:** white, solid powder; 99% purity, SHOWA Chemical Co., Ltd. and Sulfur hexafluoride (SF_6): gas, 99% SF_6 and 1% N_2, Ming Yang Special Gas Co., Ltd.

2.2. Preparation of materials

Ionic exchange was carried out at room temperature by stirring 10 g of 13X zeolite (which is the spherical tablets with diameter, ~30-35 mm) in 250 mL of aqueous solution containing $Me(NO_3)_2$ with various concentrations for 12 h. The resultant solid was filtered and washed with DI water until free of nitrate salt and dried at 120 ºC for 12 h. Subsequently, the exchanged 13X zeolite was calcined at 550 ºC for 3 h. The obtained samples are labeled as **nCoX, nNiX, nZnX and nCuX** (where n is the concentration of $Me(NO_3)_2$ solution used during the exchange process).

2.3. Characterisation

The adsorption-desorption isotherms were collected in an ASAP 2020 instrument (Micromeritics). The obtained data were analysed using the Brunauer-Emmett-Teller (BET; specific surface area) and Barrett-Joynerr-Halenda (BJH; pore diameter, pore distribution and micro- and mesopore volume) models.

The structure of the samples was investigated by X-ray diffraction (XRD) using a PANalytical X'pert PRO system. The diffraction patterns were collected using Cu Kα1 (λ = 1.54 Å) in a 2θ range of 10–80º with a step of 0.02.

Scanning electron microscope (SEM) imaging was studied with a JOEL microscope (model JSM 6330 TF) and using the energy dispersive spectroscope (EDS) analysis on SEM to calculate the atomic components of the samples.

2.4. Sulfur hexafluoride adsorption tests

2.4.1. Adsorptive apparatus and producers

Sulfur hexafluoride adsorption was carried out at room temperature using an adsorption system that was shown in Figure 1. Prior to SF_6 adsorption, the zeolite adsorbents were dried at 100 ºC for 30 min in an oven to remove moisture completely. 5 g zeolite was put into a U-shape tube with a diameter of 0.7 cm, cross-sectional area of 0.38 cm^2 and length of 38 cm. Then N_2 flow was passed through the adsorption system to remove air. The first, SF_6 flow was passed through the (A) branch to control the SF_6 concentration by N_2 flow. As the SF_6 concentration fitted and unchanged, the SF_6 flow is passed through adsorbent for the adsorption process. Honeywell analytic detector was used to determine the SF_6 concentration and adsorbed time during the adsorption process.

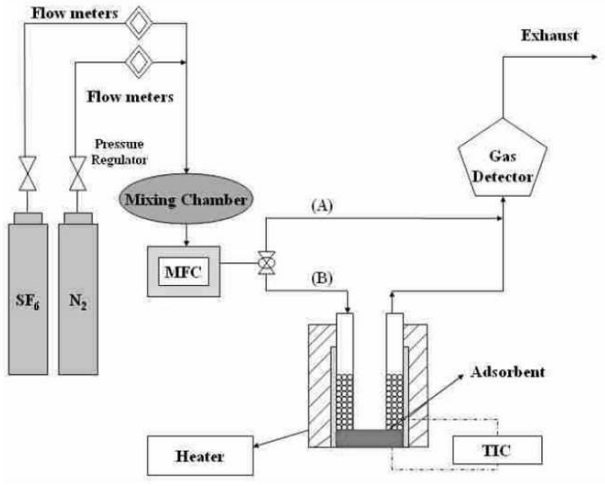

Figure 1. Scheme of the SF_6 adsorption on the exchanged 13X zeolite adsorbents

2.4.2. Calculation

The efficiency of SF_6 removal is calculated from Eq. 1:

$$\eta = \frac{C_{in} - C_{out}}{C_{in}} \quad (1)$$

Where C_{in} and C_{out} (ppm) are the initial SF_6 concentration before and external SF_6 concentration, respectively.

The volume, V (L) of adsorbed SF_6 gas is calculated:

$$V(L) = C \times r \times t \times 10^{-6} \quad (2)$$

Where C (ppm) is the SF_6 concentration, r (L min^{-1}) is the rate of SF_6 flow and t (min) is time in which SF_6 gas was adsorbed up to 99%.

The SF_6 adsorption capacity of adsorbents, q (mg g^{-1}), is determined:

$$q = \frac{\frac{V}{24.5} \times M}{m_{adsorbents}} \times 1000 \quad (3)$$

With V (L) is the volume of adsorbed SF_6 gas, M = 146.05 g/mol is molar mass of SF_6 and m (g) is the mass of adsorbent, used during the adsorption.

3. RESULTS AND DISCUSSION

3.1. Characterization of the exchanged-13X zeolite

The effect of metal ions on the crystal structure of 13X zeolite was examined using XRD. Figure 2 shows that the Faujasite framework of 13X zeolite was retained during the metal ions-exchange process. The X-ray diffraction analysis showed some different changes on the intensity and position of reflection peaks of the MeX samples with respect to the exchange of the various metal ions such as the peak at 2θ = 23.2º. The loss of crystallinity was slight for 0.10ZnX and 0.10CoX samples but more significant for 0.10NiX and 0.10CuX samples due to strong interaction of Ni^{2+} and Cu^{2+} ions with lattice oxygens. The intensity and position of the reflection peaks of 13X, 0.10CoX, 0.10ZnX zeolite samples before and after SF_6 adsorption were similar (Figures 2 and 3). So that there is not a chemical interaction between SF_6 and zeolites, therefore, the zeolite adsorbents can be used again after the SF_6 gas removal and storage.

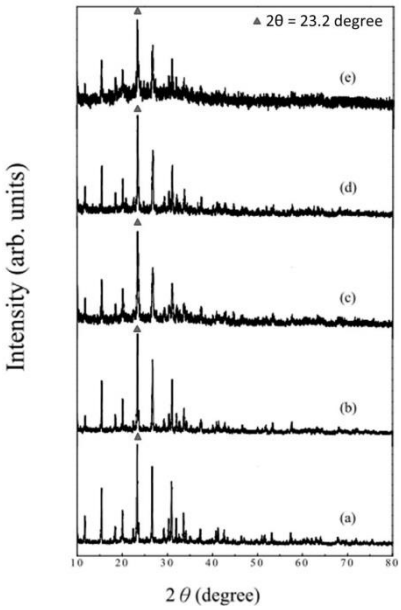

Figure 2. X-ray diffraction patterns of the zeolite samples: (a) 13X, (b) 0.1ZnX, (c) 0.1NiX, (d) 0.1CoX, and (e) 0.1CuX

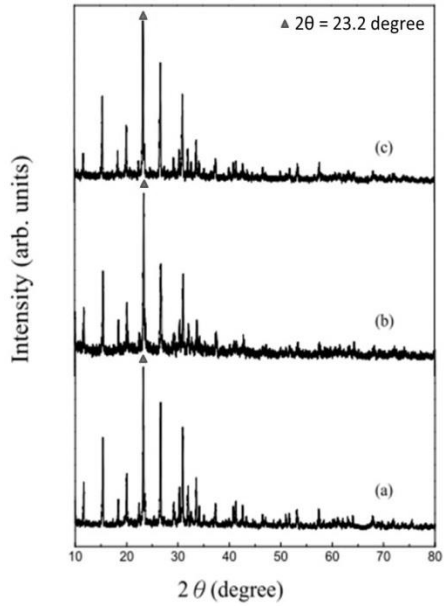

Figure 3. X-ray diffraction patterns of the zeolite samples adsorbed SF_6 gas: (a) 13X, (b) 0.1CoX, and (c) 0.1ZnX

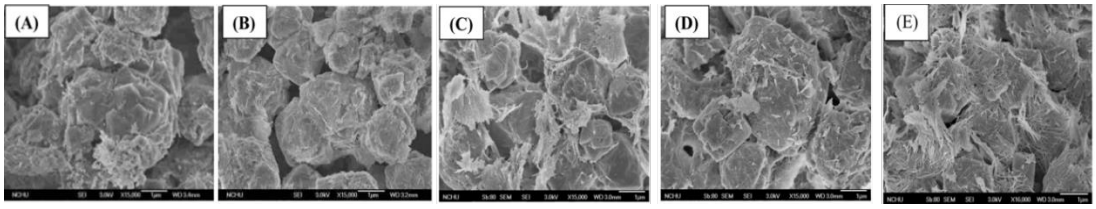

Figure 4. SEM images of the zeolite samples: (A) 13X, (B) 0.10ZnX, (C) 0.10NiX, (D) 0.10CoX and (E) 0.10CuX.

SEM image analysis indicates that the morphology of the 13X zeolite and metal ion-exchanged 13X zeolites slightly changes, all samples show nearly spherical shape crystallites of 1–3 μm in size because the metal ions exchange process only occurs in the sites containing sodium cations and not causes the significant collapse of structural cages of the 13X zeolite (Figure 4). However, the particle surfaces of the 13X (A), 0.1ZnX (B) and

0.1CoX (D) zeolites are smooth and clean, whereas the ones of the 0.1NiX (C) and 0.1CuX (E) zeolites are rough and eroded, causing the loss of regular shapes for some particles due to strong interaction of Ni^{2+} and Cu^{2+} ions with lattice oxygens. The atomic components of particle surfaces of exchanged zeolites are also determined by using EDS analysis.

Table 1. The surface are, pore volume and pore diameter of the zeolite adsorbents

Zeolites	Surface area, $S_{BET}/m^2/g$	Pore volume,$V/cm^3/g$	Pore diameter, D/nm
13X	555	0.105	19.2
0.07CoX	425	0.118	14.7
0.07ZnX	477	0.102	10.4
0.07NiX	317	0.168	8.6
0.07CuX	263	0.176	8.3

The surface area (S_{BET}), pore volume (V_{BJH}) and pore diameter (D_{BJH}) of the exchanged zeolites are measured by using BET and BJH method and listed in Table 1 and Table 2. These results will be discussed later (see sections 3.2.1 and 3.2.2).

Table 2. The SF_6 adsorption capacities and adsorbed time of the Co^{2+} and Zn^{2+}-exchanged 13X zeolites

Zeolites	Metal Quantity/%	Surface area, $S_{BET}/m^2/g$	Pore diameter, D/nm	SF_6 adsorption capacities/mg/g	SF_6 adsorbed time/min
	% Co				
0.03CoX	1.66	447	10.4	1.340	16.0
0.05CoX	---	420	11.2	1.180	18.5
0.07CoX	3.51	425	10.4	1.100	13.0
0.10CoX	4.78	393	9.1	0.960	14.8
	% Zn				
0.03ZnX	1.86	504	15.1	---	---
0.05ZnX	2.91	499	14.0	0.560	15.6
0.07ZnX	3.49	477	14.4	0.827	23.0
0.10ZnX	4.58	501	10.7	0.223	19.6

3.2. SF_6 adsorption on the zeolite adsorbents

3.2.1. Effect of metal cations on the SF_6 removal efficiency of exchanged 13X zeolites

The SF_6 removal efficiency of 13X zeolite was studied with the different SF_6 concentration of 3000, 4500 and 6000 ppm. It is long time (about 27 min) to SF_6 gas is obtained a saturated state into the 13X zeolite and the removal efficiency is 76% for 3000 ppm, 67% for both 4500 and 6000 ppm. This removal efficiency is so low, therefore, the modification of the 13X zeolite by ion-change is a great need for improving the SF_6 removal efficiency of zeolites.

Figure 5 represents the removal capacities of the metal ions-exchanged 13X zeolites with the SF_6 initial concentration of 4500 ppm. It can see that the removal efficiency of SF_6 gas was obtained up to 99% for 0.07CoX and 0.07ZnX exchanged zeolites, whereas the one of 0.07CuX and 0.07NiX exchange zeolites was 62 and 71%, respectively. So the SF_6 removal capacity of the metal ions-exchanged zeolites decreases as following CoX > ZnX > NiX > CuX zeolite due to

decreasing of surface areas (S_{BET}) and pore diameters (D_{BJH}), which were listed in Table 1. This result can be attributed to interactive properties of metal ions into the framework of zeolites that was discussed in the above characterisation. Although the surface area of 0.07ZnX zeolite is great than its 0.07CoX zeolite, the SF_6 removal capacity of 0.07CoX zeolite is higher than 0.07ZnX zeolite because pore volume and pore diameter of 0.07CoX are higher than 0.07ZnX zeolite. On the other hand, the SF_6 removal efficiency of 0.07CoX and 0.07ZnX exchanged zeolites is great than 13X zeolite because the pore diameter of 13X zeolite is so large (~19.2 nm) to compare with kinetic diameter of SF_6 (5.5 Å), thus, SF_6 gas is easily desorbed from the 13X zeolite framework leading to a decrease in the SF_6 storage capacities. Finally, the Co^{2+} and Zn^{2+} ions-exchange in the 13X zeolite leads to a significant increase in the SF_6 adsorption capacities of zeolites, whereas it slightly changes for the Ni^{2+} and Cu^{2+} ions-exchange.

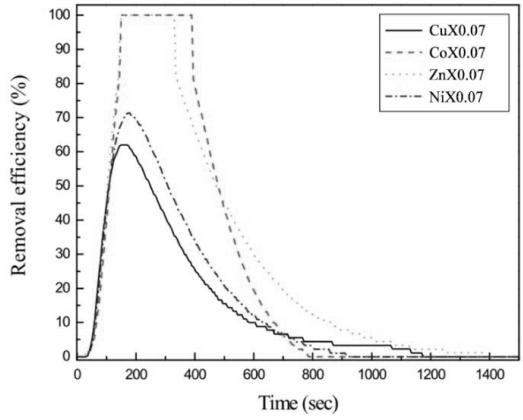

Figure 5. The SF_6 removal efficiency of metal ions-exchanged 13X zeolites with initial SF_6 concentration of 4500 ppm

3.2.2. Effect of the $Co(NO_3)_2$ and $Zn(NO_3)_2$ solution concentration on the SF_6 removal efficiency of exchanged 13X zeolites

The initial concentration effect of $Co(NO_3)_2$ and $Zn(NO_3)_2$ solutions on the SF_6 adsorption properties of zeolites was investigated with initial SF_6 concentration of 4500 ppm. The results were showed on Figure 6 and listed in Table 2.

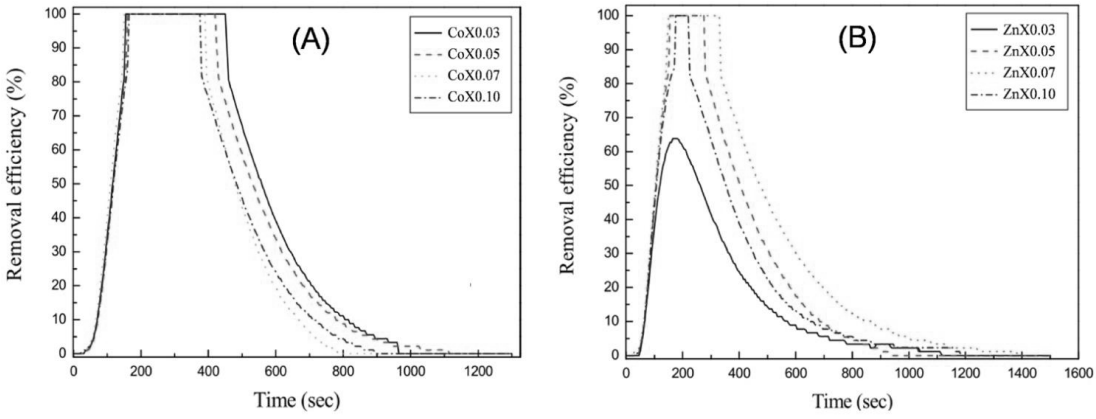

Figure 6. The SF_6 removal efficiency of the Co^{2+} and Zn^{2+}-exchanged 13X zeolites: CoXn zeolites (A) and nZnX zeolites (B), where n is the $Co(NO_3)_2$ and $Zn(NO_3)_2$ solution concentration of 0.03, 0.05, 0.07 and 0.1 M

Figure 6A indicates that the 0.03CoX zeolite has the highest interval (~ 5 min) that the SF_6 removal efficiency obtained 99%, subsequently, this interval is notated ΔT and the SF_6 adsorption capacity is achieved 1.34 mg/g. The adsorption capacities and adsorbed time were listed in Table 2. The SF_6 adsorption capacities of nCoX exchanged zeolite decrease with increasing the initial concentration of $Co(NO_3)_2$ solution due to the increase of cobalt (II) quantity in 13X zeolite framework (where n is the initial $Co(NO_3)_2$ solution concentration of 0.03, 0.05, 0.07, and 0.10 M). The representation of cobalt (II) improved the SF_6 adsorption capacity of 13X zeolites, however, as cobalt (II) quantity is so high leading to a decrease in pore diameter of zeolite framework because the cobalt (II) diameter is great than sodium diameter. Hence, the SF_6 gas was reduced the move and storage capacities into the cobalt (II)-exchanged 13X zeolite resulted in the saturation of SF_6 gas is quickly obtained in the exchanged 13X zeolites. This result consists with decreasing the surface area of exchanged zeolites.

Figure 6B shows that the SF_6 removal efficiency is 64% for 0.03ZnX exchanged zeolite and 99% for 0.05ZnX, 0.07ZnX and 0.10ZnX exchanged zeolites. The interval ΔT is about 2 min for 0.05ZnX, about 3 min for 0.07ZnX, and 42 s for 0.10ZnX exchanged zeolite. The SF_6 adsorption capacities and adsorbed time were listed in Table 2. It can see that the adsorption capacity is the highest for nexchanged zeolite (0.827 mg/g), and it significantly decreases for 0.10ZnX exchanged zeolite (0.223 mg/g) owning to the decrease in pore diameter caused by increasing zinc (II) quantity in the nZnX exchanged zeolite framework.

In conclusion, the optimal concentration that was used during the ions-exchange process is 0.03 M for $Co(NO_3)_2$ solution and 0.07 M for $Zn(NO_3)_2$ solution with the SF_6 adsorption capacity is 1.34 mg/g and 0.827 mg/g, respectively. The SF_6 adsorption capacity of the Co^{2+}-exchanged 13X zeolites is higher than Zn^{2+}-exchanged 13X zeolites. Furthermore, the interval ΔT is higher for Co^{2+}-exchanged 13X zeolite. These can be attributed the interaction between cobalt (II) and lattice oxygens that one is stronger than the interaction of zinc (II). As a result the surface of Co^{2+}-exchanged 13X zeolite is more rough and porous than ones Zn^{2+}-exchanged 13X zeolite, thus, the pore volume of Co^{2+}-exchanged zeolite is great than the pore volume of Zn^{2+}-exchanged zeolites.

3.2.3. Effect of the SF_6 concentration and the rate of SF_6 flows on the SF_6 removal efficiency of exchanged 13X zeolites

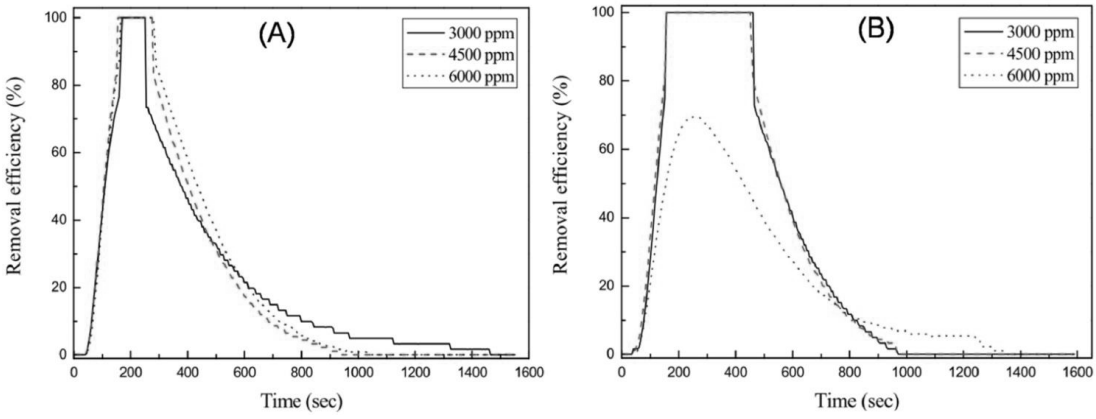

Figure 7. The SF_6 removal efficiency of the exchanged 13X zeolites with the different initial SF_6 concentrations: 0.05ZnX zeolite (A) and 0.03CoX zeolite (B).

The effect of the initial SF_6 concentration on the SF_6 removal efficiency of exchanged zeolites is studied and showed on Figure 7. For SF_6 concentration of 3000 ppm, it is 24.5 min

that the adsorbed SF_6 gas on 0.05ZnX zeolite is obtained saturated state, in which $\Delta T = 1.4$ min is the interval that the SF_6 removal efficiency achieved 99% (Figure 7A). At higher concentration (4500, 6000 ppm), there is a slight decrease in the interval ΔT and the saturation of adsorbed SF_6 gas is quickly obtained (Figure 7A). Figure 7B shows that the 0.03CoX exchanged zeolite has the interval ΔT is 5 min for initial SF_6 concentration of 3000 and 4500 ppm and simultaneously to obtain about 1.3 mg/g in the SF_6 adsorption capacities. As the SF_6 concentration is raised to 6000 ppm, the SF_6 removal efficiency is only achieved 69% owning to the difficult diffusion of SF_6 molecules into the exchanged zeolites at high SF_6 concentration. The 0.05ZnX exchanged zeolite is achieved the removal efficiency of 99% at the SF6 concentration of 6000 ppm because its pore diameter is larger than the 0.03CoX exchanged zeolite (Table 2).

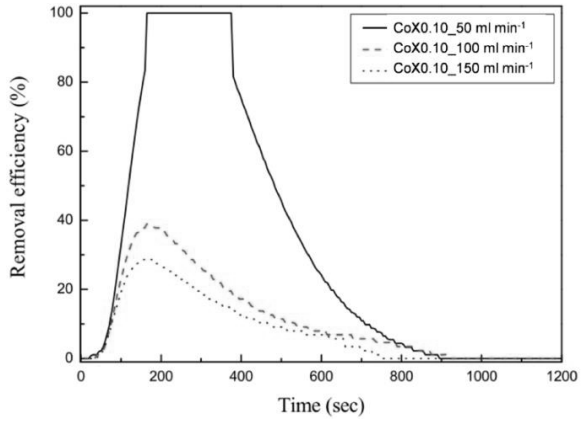

Figure 8. The SF_6 removal efficiency of the 0.10CoX zeolte with the different rate of SF_6 flows.

Figure 8 represents the SF_6 removal efficiency of the 0.10CoX zeolite with the different rate of SF_6 flows. It can see that the SF_6 removal efficiency at the SF_6 flow rates of 50, 100, and 150 mL/min is about 99%, 39%, and 29%, respectively. So, the removal efficiency decreases with increasing the rate of SF_6 flow because the storing time of SF_6 gas in adsorbed tube decreases.

4. CONCLUSION

The cationic exchange process is accompanied by a textural damage for the cation-exchanged 13X zeolites, especially, in the case of Ni^{2+} and Cu^{2+}-exchanged 13Xzeolites. The SF_6 removal capacity of the metal ions-exchanged zeolites decreases as following CoX > ZnX > NiX > CuX zeolites, in which the only Co^{2+} and Zn^{2+}-exchanged 13X zeolite are achieved 99% SF_6 removal efficiency. The SF_6 adsorption capacity is 1.34 mg/g for 0.03CoX exchanged zeolite and 0.827 mg/g for 0.03ZnX exchanged zeolite, respectively. The ZnX0.03 exchanged 13X zeolite can be obtained 99% SF_6 removal efficiency at all of SF_6 concentration of 3000, 4500 and 6000 ppm but the 0.03CoX exchanged zeolite can be only obtained 99% SF_6 removal efficiency at 3000 ppm SF_6 concentration. The SF_6 removal efficiency decreases with increasing the flow rate and it is the SF_6 flow rate of 50 mL/min that the 0.10CoX and 0.10ZnX exchanged zeolites can be achieved 99% SF_6 removal efficiency.

REFERENCES

1. Maiss M., Brenninkmeijer C. A. M. - Atomspheric SF_6: trends, sources and prospects, Environmental Science and Technology **32** (1998) 3077–3086.
2. Schneider M. - SonoVue, a new ultrasound contrast agent, European Radiology **9** (1999) S347.
3. Wong R. F. and Thompson J. T. - Prediction of the kinetics of disappearance of sulfur hexafluoride and perfluoropropane intraocular gas bubbles, Ophthalmology **95** (1988) 609.
4. Lindley A. A., McCulloch A. - Regulating to reduce emissions of fluorinated greenhouse gases, Journal of Fluorine Chemistry **126** (2005) 1457.
5. Furmaniak S., Terzyk A. P., Gauden P. A. and Kowalczyk P. - Simulation of SF6 adsorption on the bundles of single walled carbon nanotubes, Microporous and Mesoporous Materials **154** (2012) 51–55.
6. Chiang Y. C. and Wu P.Y. - Adsorption equilibrium of sulfur hexafluoride on multi-walled carbon nanotubes, Journal of Hazardous Materials **178** (2010) 729–738.
7. Carrillo I., Ramírez-de-Arellano J. M. and MaganaL. F. - Adsorption of sulfur hexafluoride on graphene and on grapheme with high titanium coverage, Computational Materials Science **84** (2014) 134–138.
8. Senkovska I., Barea E., Rodríguez Navarro J. A. and Kaskel S. - Adsorptive capturing and storing greenhouse gases such as sulfur hexafluoride and carbon tetrafluoride using metal–organic frameworks, Microporous and Mesoporous Materials **156** (2012) 115–120.
9. Kim M. B., Lee S. J, Lee C. Y. and Bae T. S. - High SF_6 selectivities and capacities in isostructural metal-organic frameworks with proper pore sizes and highly dense unsaturated metal sites, Microporous and Mesoporous Materials **190** (2014) 356-361.
10. Kim P. J., You Y. W., Park H., Chang J. S, Bae Y. S., Lee C. H. and Suh J. K. - Separation of SF_6 from SF_6/N_2 mixture using metal–organic framework MIL-100(Fe) granule, Chemical Engineering Journal **262** (2015) 683–690
11. Cao D. V., Sircar S. - Heat of adsorption of pure sulfur hexafluoride on micro-mesoporous adsorbents, Adsorption **7** (1) (2001) 73-80.
12. Murase H., Imai T., Inohara T.and Toyoda M. - Use of zeolite filter in portable equipment for recovering SF_6 in SF_6/N_2 mixtures, IEEE Transactions on Dielectrics and Electrical Insulation **11** (2004) 166.
13. Santiago Builes, Thomas Roussel and Lourdes F. V. - Optimization of the separation of sulfur hexafluoride and nitrogen by selective adsorption using monte carlo simulations, American Institute of Chemical Engineers Journal **57** (2011) 962–974
14. Hammoudi H., Bendenia S., Khelifa A. and et al. - Effect of the binary and ternary exchanges on crystallinity and textural properties of X zeolites, Microporous and Mesoporous Materials **113 (**2008) 342–351.
15. Li J., Wu E., Song J., Xiao F. and Geng C. - Cryadsorption of hydrogen on divalent cation-exchanged X zeolite, International Journal of Hydrogen Energy **34** (2009) 5458–5465.
16. Sebastian J., Peter S. A. and Jasra R. V. - Adsorption of nitrogen, oxygen, and argon in cobalt (II)-exchanged zeolite X, Langmuir **21** (24) (2005) 11220–11225.
17. Bendenia S., Marouf-Khelifa K., Batonneau-Gener I., Derriche Z. and Khelifa A. - Adsorptive properties of X zeolites modified by transition metal cation echange, Adsorption **17** (2) (2011) 361–370.

TÓM TẮT

SỰ HẤP PHỤ SULFUR HEXAFLOURIDE CỦA ZEOLITE 13X ĐÃ ĐƯỢC BIẾN TÍNH BẰNG PHƯƠNG PHÁP TRAO ĐỔI CATION KIM LOẠI

Trần Hoài Lam[1*], Quách Nguyễn Khánh Nguyên[2]
[1]*Trường Đại học Công nghiệp Thực phẩm TP.HCM*
[2]*Trường Đại học Sài Gòn*
*Email: *thlam01@cntp.edu.vn*

Các ion Na^+ trong zeolite 13X được thay thế bằng các cation Zn^{2+}, Co^{2+}, Ni^{2+} và Cu^{2+} sau khi tiến hành biến tính với dung dịch muối nitrate ở các nồng độ khác nhau. Kết quả phân tích XRD và SEM cho thấy quá trình trao đổi cation gắn liền với quá trình phá vỡ cấu trúc của 13X zeolite, đặc biệt là trường hợp của các ion Ni^{2+} và Cu^{2+}. Khả năng loại bỏ và hàm lượng hấp phụ SF_6 phụ thuộc vào loại ion kim loại, nồng độ dung dịch muối, nồng độ SF_6 cũng như tốc độ dòng khí SF_6. Theo đó, hiệu suất loại bỏ SF_6 đạt được 99% đối với mẫu biến tính bằng Co^{2+}, Zn^{2+} và hàm lượng SF_6 cao nhất là 1,34 mg/g với mẫu 0.03CoX zeolite và 0,827 mg/g với mẫu 0.05ZnX zeolite.

Từ khóa: Sulfur hexafluoride, 13X zeolite, trao đổi ion, hấp phụ, biến tính.